

Wear Study of Chicken Eggshell-Reinforced Al6061 Matrix Composites

Surendra Kumar Dwiwedi¹ · Ashok Kumar Srivastava² · Manoj Kumar Chopkar¹

Received: 31 July 2018 / Accepted: 4 November 2018 / Published online: 30 November 2018
© The Indian Institute of Metals - IIM 2018

Abstract The present work deals with conduction of wear test on Al6061/eggshell composites with load, reinforcement and sliding distance as control factors and its regression analysis. Chicken eggshell is one of the most abundant natural waste products generated in large amount by food processing industry due to its everyday consumption. This material is simply disposed in nature thus constituting environmental hazards. Commercial use of eggshells can produce lightweight materials at low cost. Therefore, being complemented with less dense calcium carbonate, it can be used as reinforcement to develop metal matrix composite using stir casting process. Reinforcement is added in the range of 2–10 wt% at an interval of 2%. Optical microstructural characterization indicated fair distribution of particles in the matrix, and 4 wt% composite exhibited best properties among all. Further addition of particles proved to be detrimental due to increase in porosity and agglomeration of particles. Wear track and debris were examined with scanning electron microscope to explain the wear process. Regression analysis helped in establishing the relationship between the control factors. Reinforcement of eggshell particles improved the wear resistance of matrix significantly as suggested by analysis of variance.

Keywords MMCs · Al6061 · Eggshell · Stir casting · Wear

1 Introduction

Focusing improvement in fuel economy, Al6061 alloy is being explored as candidate material for application in automobile components such as piston and its components, connecting rod, brake drums where sliding- and rolling-type motion is the key factor [1, 2]. This alloy demonstrates excellent mechanical properties, castability, formability and poor wear resistance in contrast [3, 4], resulting in seizure failure of mating components having relative motion. Researchers reinforced the alloy with hard and brittle ceramic materials such as SiC, Al₂O₃, B₄C, TiO₂ [5] which improved the mentioned properties considerably. But these reinforcements are associated with constraints of high density and cost [6], and the developed composites have been put on brakes for limited use. Therefore, to serve the automobile industry better, there is a need for searching or developing materials which have combined upgraded properties and low cost altogether.

Metal matrix composites have been fabricated via various routes but stir casting method tops the list in terms of cost-effectiveness, mass production, manufacturing simplicity, flexibility in handling raw materials and process parameter control [7–9]. Moreover, the particulate metal matrix composites developed via liquid metallurgy route are isotropic in nature [10]. Another way to decrease the cost of production of composite is to focus on waste materials from different fields such as agriculture and poultry, ensuring natural availability in bulk at low cost. Nowadays, fly ash [11, 12], rice husk ash [13] and chicken

✉ Surendra Kumar Dwiwedi
surendra.dwiwedi@opju.ac.in

¹ Department of Metallurgical Engineering, National Institute of Technology, Raipur, Chhattisgarh, India

² Department of Metallurgical and Materials Engineering, SOE, OP Jindal University, Raigarh, Chhattisgarh, India

eggshell are being investigated for their suitability as reinforcements.

Any type of waste becomes a threat to environment if its concentration increases excessively. Eggshell is a widely produced waste product whose use in the society is not explained much. As a result, this waste is simply discarded in the nature, contributing to pollution. The best way to utilize eggshell waste is to convert it into useful products, aiming waste management with value addition and sustainable development. It contains 95% of calcium carbonate and 5% of other organic materials [14, 15]. Researchers have highlighted the potential use of chicken eggshell in various applications, for instance, as catalyst, adsorbent and coating pigments. Al-Ghouti and Salih [16] investigated the removal of boron from aqueous solution using waste eggshell as an adsorbent material and found that functional groups C=O and Ca–O present on the surface of eggshell, were responsible for complexation with boron and its removal from water. Lunge et al. [17] utilized eggshell waste as calcium source and synthesized “Eggshell Composite” (EC) and reported it as indigenous and economic adsorbent material for fluoride removal from water. Chouhan and Sarma [18] reported that waste eggshell-derived calcium oxide was found to be an effective catalyst for the transesterification of soybean oil and resulted in 97–98% biodiesel yield at 65 °C with alcohol/oil ratio of 9:1. Ayodeji et al. [19] carried out transesterification process for the production of biodiesel from soybean oil using pure calcium oxide and calcium oxide obtained from eggshell as heterogeneous catalysts. On comparison, it was found that the yielded biodiesel revealed similar performance patterns for both the calcined eggshell catalyst and the pure CaO catalyst. Chen et al. [20] investigated the solar photo-catalytic activity of the TiO₂/eggshell composite. Yew et al. [21] calculated adhesion strength and thermal stability of acrylic coatings while using chicken eggshell (ES) as a bio-filler and concluded that even distribution of ES particles and better ES/matrix interface caused the enhancement in coating properties. It was also reported that eggshell could be used as a bio-filler in the manufacturing of low-cost polymer composites due to its bulk availability, low density and renewable aspects. Bootklad et al. [22] prepared thermoplastic starch (TPS) using compression molding in which eggshell powder (EP) was used as filler material. The properties of TPS with eggshell filler and commercial calcium carbonate (CC) filler were compared, and it was found that TPS/EP biodegraded rapidly than TPS/CC composite. Also, TPS/EP composite was better in terms of water resistance and thermal stability of the TPS than TPS/CC composite. Toro et al. [23] fabricated polypropylene-based polymer matrix composites using commercial calcium carbonate and eggshell as bio-filler. It was concluded that the latter dispersed

well in the polymer matrix due to larger surface/volume ratio as compared to the former. Young’s modulus (E) of the polymer composite improved considerably with the increment of ES content. Hassan and Aigbodion [24] fabricated Al-Cu-Mg/ES particulate composites and reported that carbonized eggshell reinforcement in the Al-Cu-Mg alloy gave better combination of properties as compared to uncarbonized ES particles. It was also concluded that ES particles up to 12 wt% could be used to enhance the properties. Chaithanyasai et al. [25] fabricated Al6061/eggshell composites by powder metallurgy route and reported improvement in mechanical properties due to good bonding between matrix and reinforcement. Buchar and Severa [26] described the nano-indentation method for determining micromechanical properties of hen’s eggshell. Balaz [27] emphasized the green and sustainable utilization of ball-milled eggshell in different fields. It was reviewed that eggshells could be used as an agent for bioceramic synthesis, drug delivery system and composite manufacturing. Sharma and Dwivedi [28] fabricated low-cost AA2014/SiC/carbonized eggshell hybrid green metal matrix composites and studied the physical behavior, specific strength and thermal expansion of hybrid composite. Anantha and Kota [29] developed eggshell-based bio-composites and studied the sorption capability of these bio-composites to remove copper from water. Boron et al. [30] reported the fabrication of composites using bio-based polyethylene matrix and eggshell as filler material. The filler adhesion was improved through chemical treatment, and then its potential to replace commercial calcium carbonate mineral as filler material was evaluated.

Based on the literature survey, it is clear that eggshell has been potentially used in different fields but very limited attention has been paid towards its engineering application, despite the fact that it is complemented with less dense calcium carbonate [17]. Utilization of eggshell for the production of lightweight material will also serve elimination of the waste from the environment.

In the present study, dry sliding friction and wear behavior of Al6061/ES composites have been carried out with load, sliding distance and reinforcement as wear control factors. In order to estimate the wear output for a given set of control factors, a regression model has been developed. It is combined with analysis of variance (ANOVA) to find out the merit of control factors, affecting the wear output significantly.

2 Materials and Methods

Al6061 alloy and chicken eggshell powder were used as matrix and reinforcement, respectively. Alloy 6061 T6 grade was purchased from Perfect Metal Works

Corporation (PMC), Bangalore, India, while eggshell wastes were collected from local market. Table 1 provides the elemental composition of aluminum alloy by weight percentage. Eggshell contains network of protein fibers, calcium phosphate, magnesium carbonate, calcium carbonate, organic substances and water [27]. The composites were fabricated by liquid metallurgy process using stir casting machine, containing 2–10 wt% of reinforcement at an interval of 2%. Thoroughly cleaned and sun-dried eggshells were pulverized using RETSCH PM400 high energy ball milling machine. The powder size analysis was done by sieve analysis, and particle size of 100–120 microns was used. All the melt-contacting surfaces were coated with high-temperature non-sticky paint. Matrix alloy was heated at 750 °C and was allowed to melt. Eggshell powder was preheated at 500 °C for 1 h before it was added into the vortex melt. The stirrer was set to rotate at 500 rpm for 10 min wherein the eggshell powder was incorporated in a controlled manner to ensure fair distribution of particles in the melt. Thereafter, the melt was casted in a preheated steel mold to produce a cast of 20 mm diameter and 200 mm length. Specimens for various tests were achieved from the core part of the cast after machining. All the composites were prepared by the same route. Sample without reinforcement was also prepared by simply melting and casting which was termed as 0 wt% composite. Schematic view and process flowchart of stir casting technique are shown in Fig. 1a, b, respectively.

The microstructural characterizations were performed on cylindrical specimens measuring 12 mm diameter and 10 mm height, obtained from core part of the machined cast. The metallographic specimen was polished mechanically using emery paper of grades 1–5. It was then subjected to velvet polishing and diamond polishing followed by etching using Keller's reagent (solution of 95 ml distilled water + 2.5 ml nitric acid + 1.5 ml hydrochloric acid + 1 ml hydrofluoric acid) where the polished specimen was immersed for 30 s in the solution. The micrographs were captured on optical microscope (model: AxioCam ERc5 s, ZEISS).

The H scale hardness value of composites was recorded directly from Rockwell tester (model: 7005 RHT-D) with a 3.175 mm steel ball indenter. ASTM G99-standardized dry sliding wear tests were conducted on computerized pin-on-

disk machine (model: DUCOM TR20), which is shown in Fig. 1c. It recorded wear as height loss in micron, frictional force and coefficient of friction (CoF) directly in the form of screen outputs. Figure 1e, f portrays wear test specimens of 10 mm diameter and 25 mm height, which were tested against 220 grit silicon carbide (SiC) emery paper, adhered to the steel disk using a paper holder arrangement as shown in Fig. 1d. The tests were performed in ambient room conditions at different loads of 10 N, 20 N and 30 N, track of 65 mm diameter and speed of 300 rpm. The pin was pressed against the emery paper under the load for a period of 120 s. Wear loss was expressed as volume loss (mm^3) which was calculated by multiplying height loss with cross-sectional area (mm^2) of pin. Wear rate was taken as ratio of volume loss to the sliding distance. The graphs of cumulative volume loss (CVL) and wear rate (WR) were plotted against sliding distance. The wear surfaces and wear debris were analyzed using scanning electron microscopy (model: X-max 20, ZEISS) equipped with Oxford Instrument Energy Dispersive Spectroscopy (EDS).

3 Results and Discussion

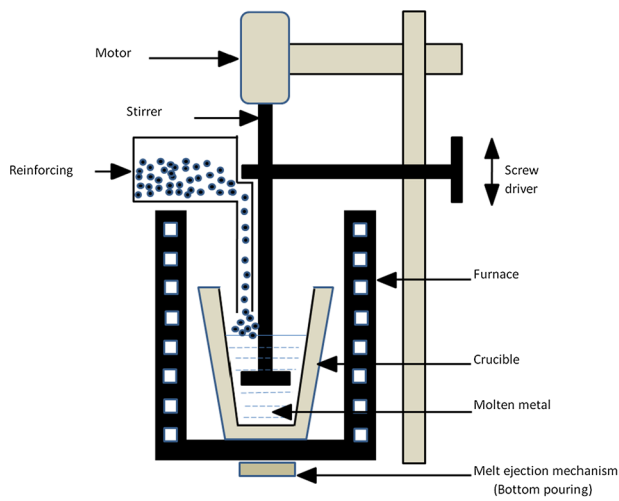
3.1 Microstructural and Mechanical Analysis

The details of microstructural and mechanical characterization of the fabricated composites have already been reported in our previous work [31]. The optical images of matrix alloy and different composites are shown in Fig. 2a–d, respectively.

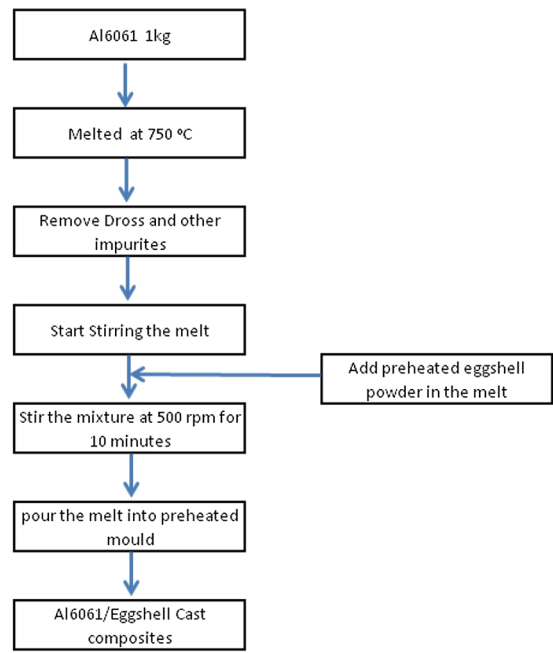
Figure 2a reveals the microstructure of unreinforced alloy matrix, marked with grain boundaries and precipitation along grain boundaries. Figure 2b depicts microstructure of 4 wt% composites which illustrates uniform distribution of eggshell particles in the matrix along with some porosity. These pores are developed due to gas entrapment and are attributed to time and speed for which stirring has been carried out [32]. Greater time and speed cause the turbulent effect of atmospheric gases over the melt and force them to get entrapped. Further, the porosity effect becomes dominant in the composites due to agglomeration and low wettability effect at increased reinforcement content [12], as demonstrated in Fig. 2c, d.

Table 1 Elemental composition of Al6061 by weight percentage

Element	Si	Fe	Cu	Mn	Mg	Cr	Zn	Ti	Al
Percentage	0.663	0.543	0.347	0.058	0.881	0.273	0.069	0.052	Balance



(a)

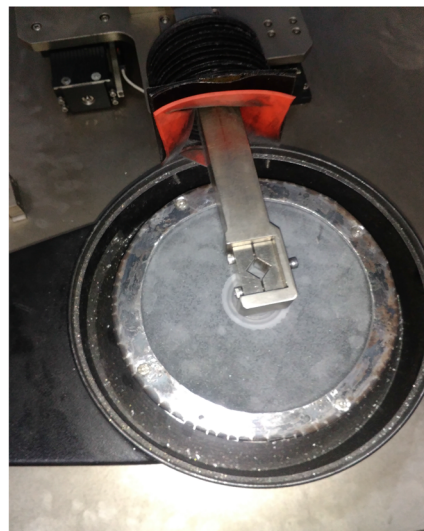


(b)



Emery Paper with Paper Holder arrangement

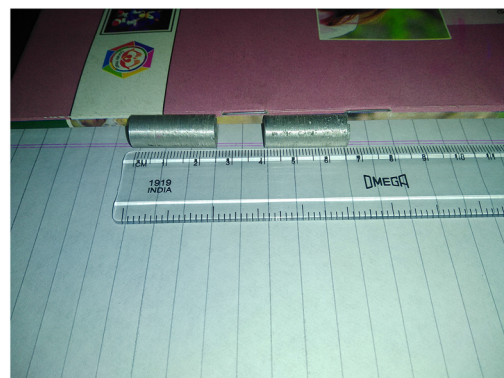
(c)



(d)



(e)



(f)

◀ **Fig. 1** **a** Schematic view of stir casting machine, **b** stir casting process flowchart, **c** pin-on-disk wear testing machine, **d** disk facilitated with emery paper holder arrangement **e** and **f** wear cylindrical samples

test attempt. Final hardness value is taken as an average of five attempts. Figure 3 shows the variation of hardness of alloy matrix and different composites.

3.2 Wear Analysis

The hardness value of alloy matrix and composites has been captured directly on Rockwell hardness testing machine. Table 2 shows the recorded values against each

Dry wear tests have been conducted against constant speed of 300 rpm, single track diameter of 65 mm to get sliding

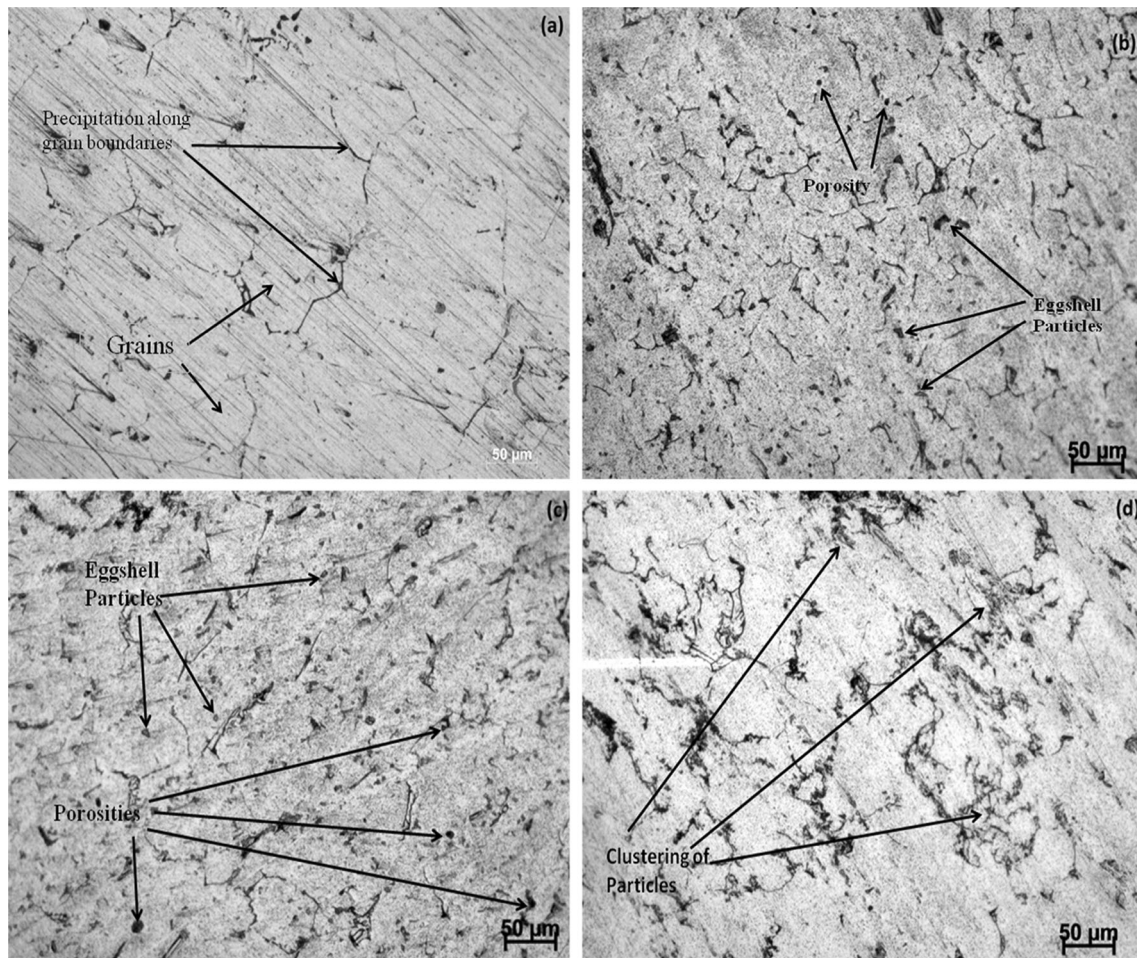


Fig. 2 Optical micrographs of **a** 0 wt%, **b** 4 wt%, **c** 6 wt.% and **d** 10 wt% composites [31]

Table 2 Rockwell hardness test results

Material	Trial 1	Trial 2	Trial 3	Trial 4	Trial 5	Average value
Alloy + 0 wt%	62	56	62	60	66	61
Alloy + 2 wt%	68	76	73	79	81	75
Alloy + 4 wt%	78	74	80	84	76	78
Alloy + 6 wt%	65	68	75	77	74	72
Alloy + 8 wt%	64	71	74	67	62	68
Alloy + 10 wt%	60	70	58	72	63	65

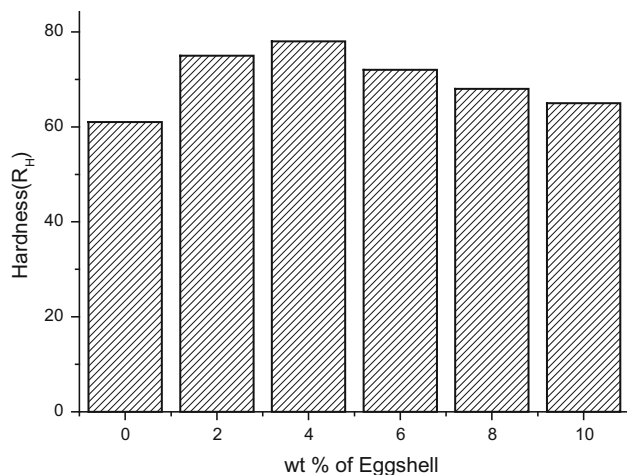


Fig. 3 Variation of hardness for different composites

velocity of 1.021 m/s and sliding distance of 122 m when rotated for 120 s.

Figure 4a–f exemplifies the graphs plotted for cumulative volume loss (mm^3) and wear rate (mm^3/m) versus sliding distance (m), respectively, for different wt% composites at three different loads. Clearly, the volumetric wear loss (Fig. 4a) increases with increase in sliding distance for both matrix and composites at a given load. It is due to the fact that sliding action between contacting surfaces of sample pin and abrasive SiC particles for longer time causes rise in temperature of matrix material. It is reported that increase in surface temperature causes matrix softening which is responsible for enhanced volume loss [33, 34]. The volumetric wear loss and wear rate are highest for the matrix while lowest for 4 wt% composite. This can be attributed to increase in hardness of composite and reduction in effective contact between abrasive particles and matrix due to presence of hard reinforcement. Rao et al. [2] explained the contacting mechanism between two sliding surfaces, which leads to the formation of mechanically mixed layer (MML). This layer strongly shields the composite surface from severe wear. As a result, effective contact between surfaces is reduced and wear loss of composites is significantly less than unreinforced alloy. Mondal et al. [35] reported that increase in hardness due to particle addition causes reduction in sticking tendency of composite surfaces with counter-surface as compared to

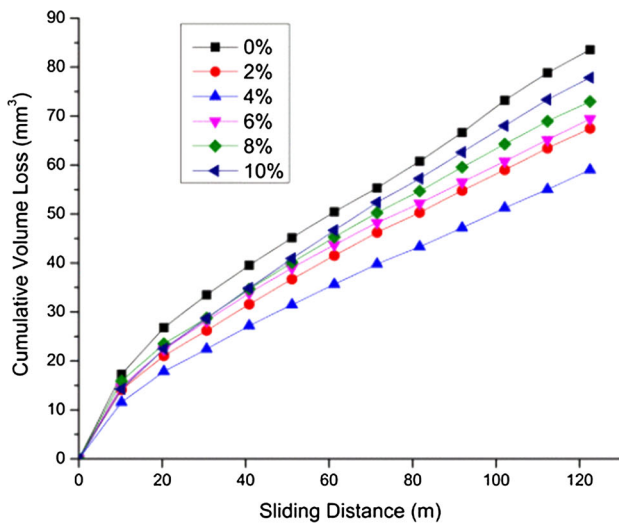
Fig. 4 Variation of cumulative volume loss (a–c) and wear rate (d–f) at 10, 20 and 30 N, respectively, for different composites as a function of sliding distance

alloy. Therefore, addition of reinforcement particles have improved the wear resistance of matrix alloy considerably.

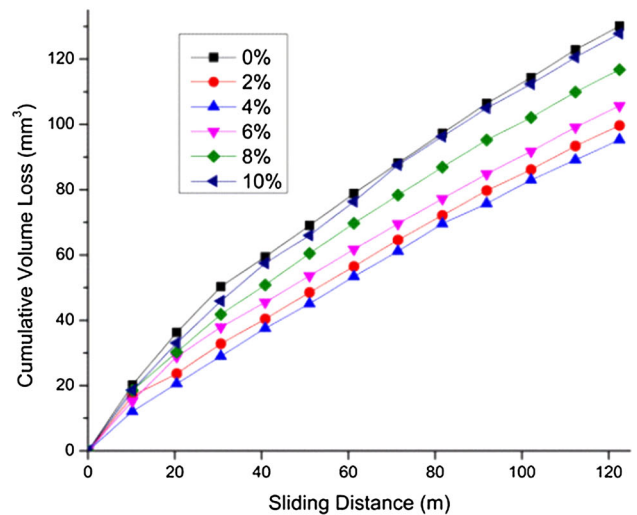
Figure 4d–f represents the wear rate variation of composites with sliding distance at different loads. Initially, the wear rate is very high for matrix and composites but later it decreases sharply and varies almost steadily. High wear rate can be attributed to hardness difference between hard SiC abrasive particle and soft matrix which causes easy penetration of hard particles under load. However, in later stage, wear rate varies steadily and this can be attributed to surface hardening effect and presence of wear debris. The excessive plastic deformation with increase in sliding distance results in strain hardening of the surface due to which wear rate decreases [36]. The presence of wear debris between contacting surfaces plays significant role in reducing the wear rate in two ways. Firstly, their presence reduces effective contact between specimen and abrasive particles. Secondly, these wear debris act as third-body abrasive which undergoes rolling effect and makes the wear process steady [34, 37].

The volumetric wear loss with variation in load is shown in Fig. 5. Volumetric loss increases with increase in load for matrix and all composites. Increase in load has caused more smearing effect of hard SiC particles in the soft matrix and thus brought delamination and plowing. As the load increases, the fine scratches have converted into deep grooves, indicating increased volumetric wear loss and wear rate.

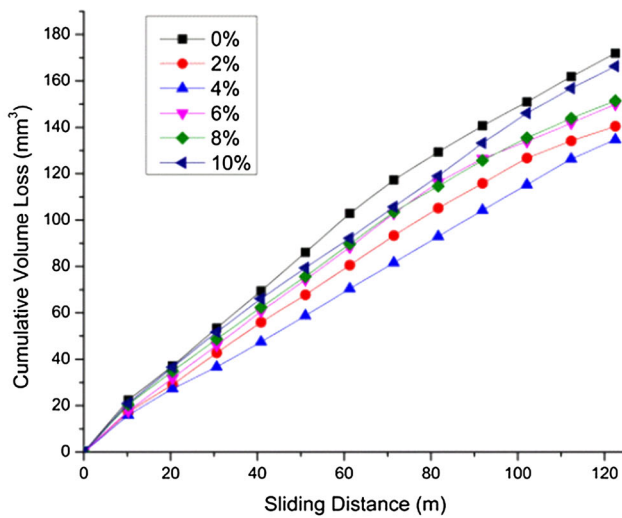
SEM micrographs of worn surfaces are shown in Fig. 6a–f, representing morphology of wear surface at loads 10 N and 30 N. It is evident from the images that morphology has changed from gentle to severe plastic deformation with increase in load, either due to plowing or delamination. Figure 6a, b reveals that matrix material has undergone finer to deeper abrasive grooving when load has increased. However, Fig. 6c, d illustrates that the wear morphology has changed for 4 wt% composites from plowing to delamination and damaged spots to craters. It is attributed to increase in hardness and brittleness of the composite. The morphology of 10 wt% composite is



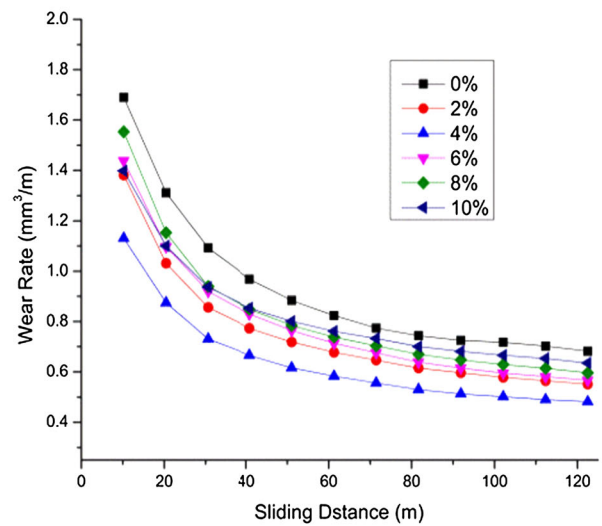
(a)



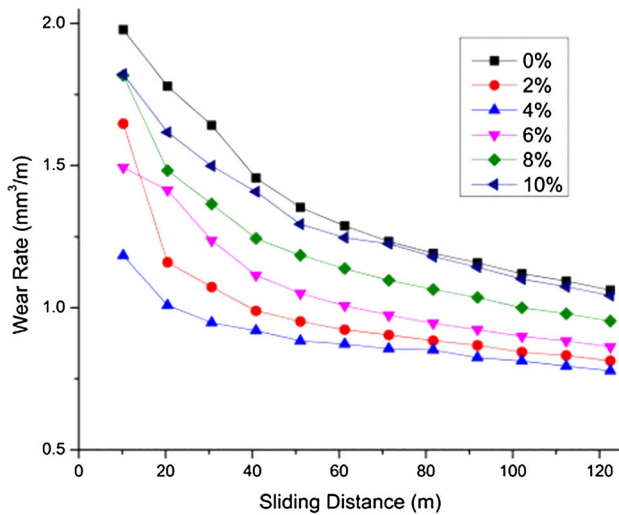
(b)



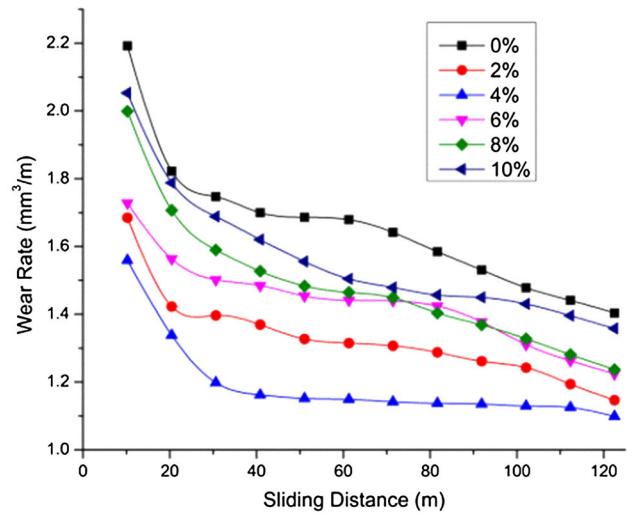
(c)



(d)



(e)



(f)

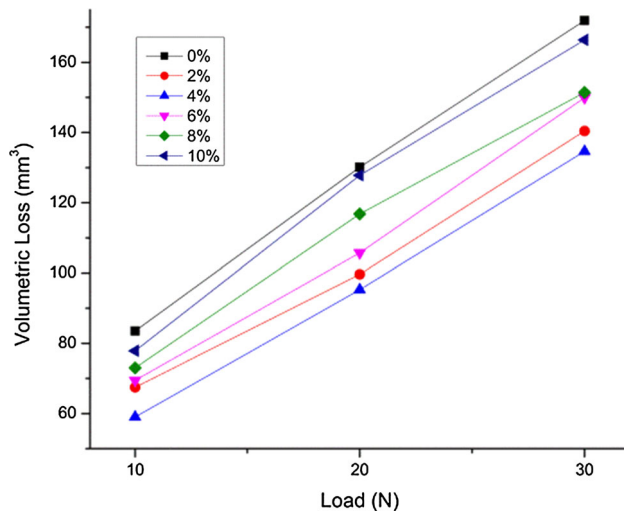


Fig. 5 Variation of volumetric loss (wear) with load for different composites

similar to matrix alloy. Figure 6e portrays excessive particle detachment and debonding, attributed to poor bonding of reinforcement with matrix and inability to bear load, while Fig. 6f shows deep plowing effect of matrix. It is clear that severity of plowing and delamination depends upon the load and hardness of material and explains the most suitable reason for low wear rates of composites.

A dry tribological study covers both wear and friction; wear by far is most significant. However extensive studies on friction and wear often lack the depth [38]. In general, both wear resistance and friction coefficient are not considered as intrinsic material properties due to their dependence on many external factors. Coefficient of friction measures the frictional force which is responsible for heat generation at the contacting surfaces. This leads to rise in temperature and softening of materials ultimately leading to increased wear loss. CoF is expected to be low in the context of automotive application where power generation and transmission are of prime objectives. Figure 7a–c shows the variation in coefficient of friction of alloy and composites with sliding distance at different loads. The coefficient of friction decreases with increase in load. Increase in load results in high wear rate of composites which suggests that

surface grip between specimen and abrasive particles stay active for very less time before it breaks. This explains that the wear rate and frictional resistance are inversely correlated. Similar findings have been reported by researchers in their previous work [36, 39].

Composite with 0 wt% and 4 wt% reinforcement exhibit maximum and minimum values of CoF at all testing loads. The possible reason for this is the hardness difference among the composites. Softer surface permits more smearing effect of abrasive particles, suggesting restricted motion with higher CoF value. The outcome is just opposite in case of hard surface as smearing effect is reduced due to the presence of hard reinforcing particles. It is also observed that CoF first increases, remains steady in the middle stage and decreases later. The effective number of abrasive particles participating in the wear process decreases remarkably either due to debonding of SiC particles or dullness of sharp edges of the abrasives. Such particles does not offer any resistance and thus CoF decreases.

Figure 8a, b represents the SEM micrograph and EDX of wear debris collected after wear test. The SEM micrograph illustrates that wear debris consists of mixture of fine particles and ribbons of composite. Fine particles have resulted due to continuous rubbing action of surface while ribbons are produced due to plowing of matrix by hard abrasive SiC particles. EDX represents the elemental analysis of wear debris which consists of composite components and loose SiC particles and thus confirms the debonding of abrasive particles from the emery paper.

3.3 Regression Modeling

Experimental results show that wear performance of composites depend on weight percentage of reinforcement (R), load (L) and sliding distance (SD). However, it is not clearly determined that which parameter is affecting the performance significantly and in which order. Therefore, these control parameters have been analyzed through Minitab 17 software using ANOVA and regression analysis.

ANOVA is helpful in determining the factors affecting the response significantly. Generally, decision is made on the basis of calculated Fisher's value (F) and the factor is

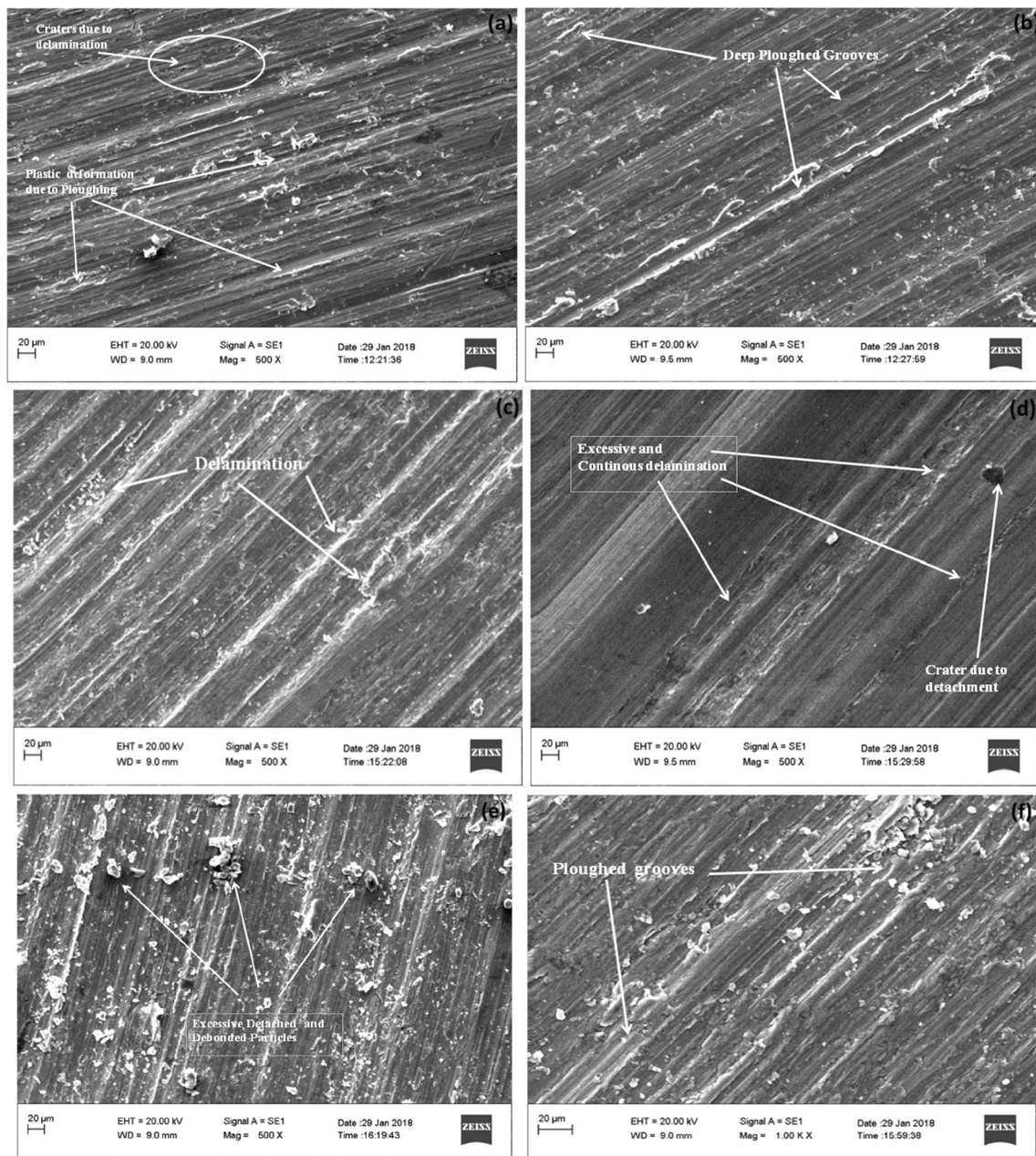


Fig. 6 SEM images of wear track of **a, b** 0 wt% **c, d** 4 wt% **e, f** 10 wt% composite at 10 N and 30 N, respectively, after sliding distance of 122 m

said to be significant, if $F > 4$ [40]. Here, cumulative volume loss (V) and wear rate (WR) are taken as wear response. ANOVA analysis demonstrated in Tables 3 and 4 shows that the wear responses are significantly affected by all the parameters; load and sliding distance top the ranking, respectively, for wear rate and volume loss. The value under the column head “Contribution” gives an idea of percentage by which the factor affects the response. This analysis evidences that reinforcement of eggshell has

significant impact on the wear performance of composites as its registered values of F for responses for V and WR are 16.66 and 61.54, respectively.

Linear multiple regression analysis has been carried out to develop a model in order to establish the correlation among control factors. The model has been developed for both the wear responses which are as follows:

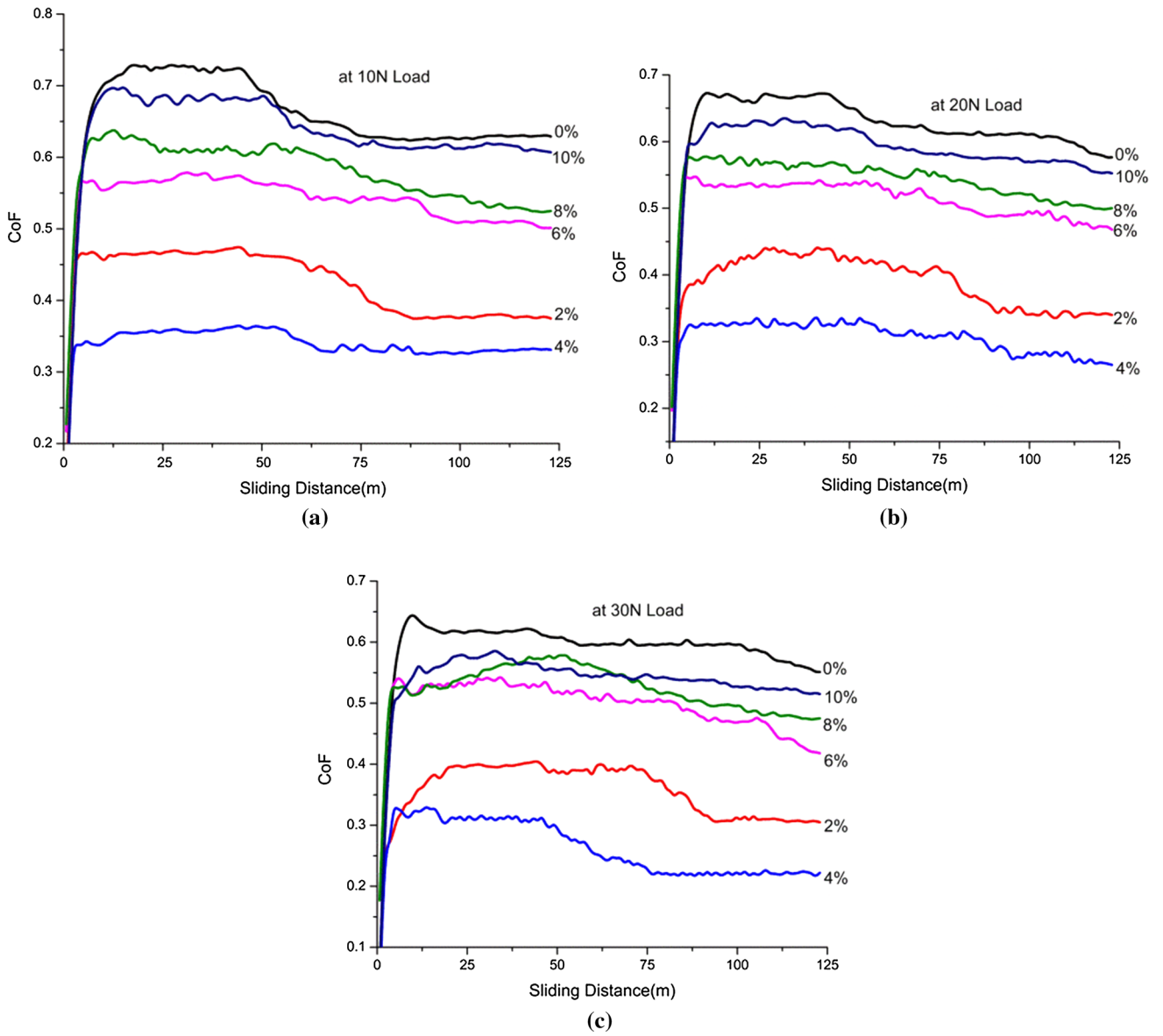


Fig. 7 Variation of CoF of different composites at a 10 N b 20 N and c 30 N with sliding distance

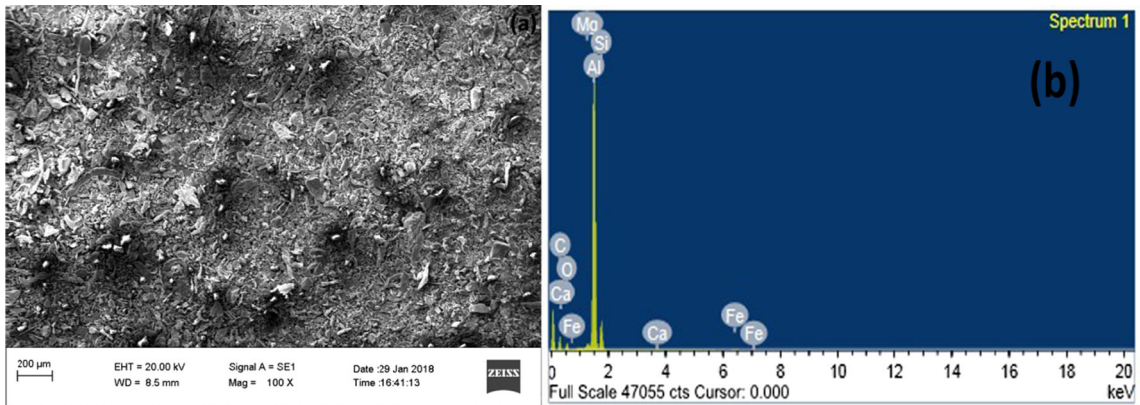


Fig. 8 a SEM and b EDX of wear debris of 4 wt% composite

Table 3 Analysis of variance for volume loss (V)

Source	DF	Seq SS	Contribution (%)	Adj SS	Adj MS	F-value	P value
Regression	3	54167	91.88	54167	18055.6	154.66	0.000
R	1	1944	3.30	1944	1944.5	16.66	0.000
L	1	22238	37.72	22238	22238.2	190.48	0.000
SD	1	29984	50.86	29984	29984.3	256.83	0.000
Error	41	4787	8.12	4787	116.7		
Total	44	58954	100.00				

Table 4 Analysis of variance for wear rate (WR)

Source	DF	Seq SS	Contribution (%)	Adj SS	Adj MS	F-value	P value
Regression	3	4.2367	94.66	4.2367	1.41223	242.03	0.000
R	1	0.3591	8.02	0.3591	0.35909	61.54	0.000
L	1	3.4608	77.31	3.4608	3.46049	593.06	0.000
SD	1	0.4171	9.32	0.4171	0.41711	71.49	0.000
Error	41	0.2392	5.34	0.2392	0.00583		
Total	44	4.4759	100.00				

Table 5 Confirmation test

Exp. no	Reinforcement % (R)	Load (L)	Sliding distance (SD)	Exp. volume loss	Model volume loss	Error %	Exp. WR	Model WR	Error %
1	2	20	122	99.65	102.336	– 2.69	0.8133	0.7694	5.40
2	2	30	122	140.456	129.566	7.75	1.1463	1.1090	3.26
3	4	20	122	95.291	106.98	– 12.27	0.7757	0.8325	– 7.05
4	6	30	122	149.94	138.862	7.38	1.2282	1.2353	– 0.58
5	8	20	100	101.105	98.892	2.18	1.0112	1.0237	– 2.26
6	10	30	100	141.294	130.77	7.44	1.4306	1.4265	0.29

$$V = -53.20 + 2.324R + 2.723L + 0.7904SD$$

$$WR = 0.3867 + 0.03158R + 0.03396L - 0.002948SD$$

The correlation coefficient (R^2) for cumulative volume loss (V) and wear rate (WR) is 0.9188 and 0.9466. The developed regression models are further validated by conducting confirmation tests, and both model and experimental values have been compared for error calculation with a set of different control factors mentioned in Table 5. The model and experimental wear responses have been compared for error calculation. It is observed that both the models are comparable and responses are close in values with minimum errors.

4 Conclusion

The present paper reports the investigation results of dry sliding wear test of Al6061/eggshell composites, fabricated by simple stir casting process. Experimental work reveals that wear resistance and coefficient of friction decreases with increase in load. Reinforcement of eggshell particles improves the wear resistance of matrix material. 4 wt% composite displays best wear resistance properties among all. Regression analysis reveals that the volumetric loss is highly affected by load followed by sliding distance and reinforcement in order. The wear rate is also dominated by load but reinforcement evolves out as more significant parameter than sliding distance. Confirmation test validates

the regression model with error falling in the range of – 12% to + 10%.

References

- Ramesh C S, Khan A R A, Ravikumar N, and Savanprabhu P, *Wear* **259** (2005) 602.
- Rao R N and Das S, *Mater Des* **32** (2011) 1066.
- Maurya R, Kumar B, Ariharan S, Ramkumar J, Balani K, *Mater Des* **98** (2016) 155.
- Umanath K, Palanikumar K, and Selvamani S T, *Compos B* **53** (2013) 159.
- Dou Y, Liu Y, Liu Y, Xiong Z, and Xia Q, *Mater Des*, **60** (2014) 669.
- Phanibhushana M V, Chandrappa C N, and Niranjana H B, *Mater Today Proc* **4** (2017) 3484.
- Pazhouhanfar Y and Eghbali B, *Mater Sci Eng A* **710** (2018) 172.
- Suresh S and Moorthi N S V *Procedia Engg* **64** (2013) 1183.
- Dinakaran I, Nelson R, Vijay S J and Akinlabi E T, *Mater Charact* **118** (2016) 149.
- Sahin Y and Kilicli V, *Wear* **271** (2014) 2766.
- Rohatgi P K, Daoud A, Schultz B F, and Puri T, *Compos A Appl Sci Manuf* **40** (2009) 883.
- Rajan T P D, Pillai R M, Pai B C, Satyanarayana K G, and Rohatgi P K, *Compos Sci Technol* **67** (2007) 3369.
- Saravanan S D and Kumar M S, *Procedia Eng* **64** (2013) 1505.
- Nakano T, Ikawa N, and Ozimek L, *Poult Sci* **82** (2003) 510.
- Krithiga G and Sastry T P, *Bull Mater Sci* **34** (2011) 177.
- Al-Ghouti M A and Salih N S, *J Mol Liquids* **256** (2018) 599.
- Lunge S, Thakre D, Kamble S, Labhsetwar N, and Rayalu S, *J Hazard Mater* **237–238** (2012) 161.
- Chouhan A S and Sarma A, *Renew Sustain Energy Rev* **15** (2011) 4378.
- Ayodeji A A, Modupe O E, Rasheed B and Ayodele J M, *Data Brief* **19** (2018) 1466.
- Chen X, Li C, Wang J, Li J, Luan X, Li Y, and Xu R, Wang B, *Mater Lett* **64** (2010) 1437.
- Yew M C, Sulong R N H, Yew M K, Amalina M A, and Johan M R, *Sci World J* **2014** (2014) Article ID: 805094.
- Bootklad M and Kaewtatip K, *Carbohydr Polym* **97** (2013) 315.
- Toro P, Quijada R, Yazdani-pedram M, and Arias J L, *Mater Lett* **61** (2007) 4347.
- Hassan S B and Aigbodion V S, *J King Saud Univ Eng Sci* **27** (2015) 49.
- Chaithanyasai A, Vakchore P R, and Umasankar V, *Procedia Eng* **97** (2014) 96.
- Buchar J and Severa L, *J Food Eng* **101** (2010) 146.
- Balaz M, *Adv Colloid Interface Sci* **256** (2018) 256.
- Sharma S and Dwivedi S P, *J Hazard Mater* **333** (2017) 1.
- Anantha R K and Kota S, *Groundw Sustain Dev* **7** (2018) 265.
- Boronat T, Fombuena V, Garcia-Sanoguera D, Sanchez-Nacher L, and Balart R, *Mater Des* **68** (2015) 177.
- Dwiwedi S K, Srivastava A K, Sugimoto K, and Chopkar M, *Open J Met* **8** (2018) 1.
- Ezatpour H R, Sajjadi S A, Sabzevar M H, Sabzevar M H, and Huang Y, *Mater Des* **55** (2014) 921.
- Qin Q D, Zhao Y G, and Zhou W, *Wear* **264** (2008) 654.
- Veeresh Kumar G B, Rao C S P, and Selvaraj N, *Compos B* **43** (2012) 1185.
- Mondal D P, Das S, Rao R N, and Singh M, *Mater Sci Eng A* **402** (2005) 307.
- Srivastava A K and Das K, *Tribol Int* **43** (2010) 944.
- Maxwell Rejil C, Dinakaran I, Vijay S J, and Murugan N, *Mater Sci Eng A* **552** (2012) 336.
- Dumbleton J H, In: *Tribology of Natural and Artificial Joints*, vol 3, Elsevier (1981) 460 p.
- Uyyuru R K, Surappa M K, and Brusethaug S, *Tribol Int* **40** (2007) 365.
- Prakash K S, Kanagaraj A, and Gopal P M, *Trans Nonferrous Met Soc China* **25** (2015) 3893.